

A CHANDRA OBSERVATION OF THE DIFFUSE EMISSION CENTERED ON THE LOW MASS X-RAY BINARY 4U 1755–33

SHINAE Q. PARK¹, JON M. MILLER^{1,2}, JEFFREY E. MCCLINTOCK¹, STEPHEN S. MURRAY¹

Draft version September 14, 2018

ABSTRACT

We present an analysis of a *Chandra* observation of the field surrounding the low-mass X-ray binary 4U 1755–33, which has been in quiescence since 1996. In 2003, Angelini & White reported the appearance of a narrow 7' long jetlike feature centered on the position of 4U 1755–33 using the *XMM-Newton* telescope. Though the source and jet are not visibly apparent in our *Chandra* ACIS-S image, there is a significant excess (4–6 σ) of counts in a region that encloses the jet when compared to adjacent regions. We examined a knot of emission in the jet that was detected by *XMM-Newton* but not by *Chandra* and calculated that if the knot flux observed by *XMM-Newton* was concentrated in a point source, *Chandra* would have easily detected it; we therefore conclude that this knot of emission is diffuse. In summary, we suggest that the jetlike feature found previously in the *XMM-Newton* data is quite diffuse and likely a true jet, and is not due to a chance alignment of discrete point sources or point-like regions of emission associated with internal shocks.

Subject headings: binaries: close — X-rays: stars — stars: individual (V4134 Sagittarii, 4U 1755–33)

1. INTRODUCTION

4U 1755–33 is a low-mass X-ray binary (LMXB) and black hole candidate located in the direction of the Galactic center. It was first discovered by the *Uhuru* satellite's all-sky X-ray survey in 1970 (Giacconi et al. 1974) with a flux of $\sim 100\mu\text{Jy}$. The X-ray source remained bright and persistent until January 1996, when the *Rossi X-ray Timing Explorer* (*RXTE*) failed to detect the source while in its off state with a flux of $\leq 1\mu\text{Jy}$ (Roberts et al. 1996). The source has remained quiescent since then, to the time of writing.

The X-ray spectrum of 4U 1755–33 indicates that the primary may be a black hole. The spectrum was observed to be “ultrasoft” ($kT \sim 2$ keV) when the source was bright (Jones 1977; White & Marshall 1984a; White et al. 1984b), and a hard X-ray tail above $\sim 6 - 10$ keV was observed by Pan et al. (1995); both spectral aspects are frequently observed for black hole candidates (Tanaka & Lewin 1995). Seon et al. (1995) also noted the appearance of an iron emission line centered around 6.7 keV, as found in many black hole candidates (Miller et al. 2002a,b; Park et al. 2004).

The optical counterpart of 4U 1755–33 was identified as a faint, blue star with a featureless spectrum by McClintock et al. (1978). When the X-ray source was active, the optical counterpart was a $V \sim 18-19$ mag object. Since turning off, the counterpart has dimmed to $V > 22$ (Wachter & Smale 1998). A regular, periodic dipping in the X-ray light curve of the source was observed by White & Marshall (1984a), suggesting that the source is being observed at a high inclination angle. This periodicity also allowed for the determination of the 4.4 hr orbital period of the binary (White et al. 1984b), a result confirmed by the photometric variations

in the optical counterpart by Mason, Parmar, & White (1985). This period, along with the period-mass relation (Frank, King, & Raine 2002), suggests a mass of $\sim 0.5 M_{\odot}$ for the secondary star. The distance to this source is thought to be between 4–9 kpc (Wachter & Smale 1998).

In 2003, Angelini & White reported the *XMM-Newton* discovery of an X-ray-emitting jetlike feature that is 7' in extent, narrow, and centered at the position of 4U 1755–33. They suggest that it has existed since the source entered quiescence. The 3/5 half-length of the jet corresponds to 4 pc for an assumed distance of 4 kpc. Thus, as Angelini & White note, it is plausible that a relativistic jet could have expanded to this length, given that the source was active for at least 25 years. They also report the existence of a hole developing near the LMXB, which is consistent with the scenario that the source has not been feeding the jet during the past eight years of quiescence. Although jets are not seen exclusively in black holes binaries, they are relatively common in such systems (e.g. Mirabel 2003). Confirmation that this extended X-ray emission feature is a true jet would provide further evidence that 4U 1755–33 may contain a black hole primary. In this Letter, we present a *Chandra* observation of 4U 1755–33 and report on the diffuse appearance of the jetlike feature.

2. OBSERVATIONS AND ANALYSIS

We observed 4U 1755–33 with the *Chandra* X-ray Observatory on 2003 September 25 from 17:21:18 to 23:51:50 UT, with 21909 s of good time exposure. The incoming X-ray flux was read out by the Advanced CCD Imaging Spectrometer (ACIS) spectroscopic array (ACIS-S) with the very faint format in timed exposure mode. At the time of the proposal, it was not known that 4U 1755–33 might have a jetlike feature extending from it, and thus the source was placed at the standard aimpoint near the boundary between nodes 0 and 1 on the ACIS-S3 CCD chip. This aimpoint is not at the center of chip, so unfortunately, the S3 CCD did not capture the full length

¹ Harvard-Smithsonian Center for Astrophysics, 60 Garden Street, Cambridge, MA 02138; spark@cfa.harvard.edu, jmmiller@cfa.harvard.edu, jmclintock@cfa.harvard.edu, smurray@cfa.harvard.edu

² NSF Astronomy and Astrophysics Fellow

of the region of extended emission. In order to avoid measurement errors due to the very different responses of the S3 and S2 chips, we chose to only look at ACIS-S3, cutting off about 15% of the region in question (see Fig. 1).

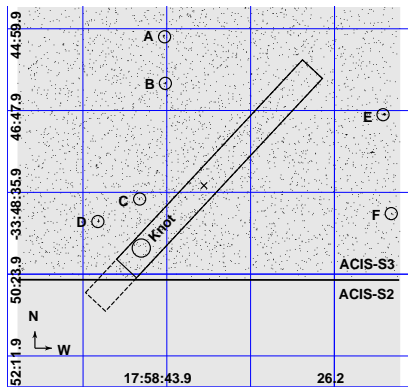


FIG. 1.— *Chandra* ACIS-S3 chip image of the 4U 1755–33 region in the 0.3–7.0 keV band. The full rectangular region of length $7'$ in the center of the image shows the extent of the jetlike emission observed by Angelini & White (2003) with *XMM-Newton*; the central “x” denotes the position of 4U 1755–33. In the *Chandra* analysis, we consider only the upper $6'$ of the emission (solid line) that was imaged by the ACIS-S3 chip. The circle within the rectangular region encloses the location of the knot-like feature observed by *XMM-Newton*. Neither this feature nor the jet itself is apparent in a visual inspection of the ACIS-S3 image. The smaller circles denoted by A–F are point sources detected by both *Chandra* and *XMM-Newton*.

We compare the *Chandra* data with the *XMM-Newton* data for the same source, which were taken on 2001 March 8 in a 5 hour exposure using the two EPIC-MOS arrays operated in full frame mode and the EPIC-PN array in extended full frame mode (Angelini & White 2003). All three cameras observed the source with the “medium” optical blocking filter. The good time exposure in each camera was 18127 s, 18107 s, and 15359 s for the MOS-1, MOS-2, and PN cameras respectively.

The *Chandra* data were analyzed using standard processing tools from CIAO version 3.0.2. No significant flaring was seen in the data, and the response files used were corrected for the gradual degradation in the low-energy response of the ACIS detector. We also reanalyzed the *XMM-Newton* data obtained through the HEASARC public data archive using the *XMM-Newton* Science Analysis System (SAS) version 5.4.1 to undertake a proper comparison of the data between the two telescopes. Because the PN camera has less uniform coverage due to the gaps between the CCDs and bad pixel columns, we chose to use only the data from the two MOS cameras in our analysis. The difference in sensitivity between these two cameras is modest, and in our results we found that the MOS-2 camera yielded greater flux values by at most 15%. For our analysis, we quote only the average of the two cameras.

The spectra of the data from both *Chandra* and *XMM-Newton* were binned to contain a minimum of 15 counts in each channel and analyzed in the 0.3–7.0 keV band using XSPEC version 11.2 (Arnaud & Dorman 2000). The region of the jetlike feature was specified to be $7'$ in length by Angelini and White, and estimated by us to be 0.6 in width from the *XMM-Newton* images. Because

a feature $7'$ in length centered on the source does not fit in the *Chandra* ACIS-S3 chip, we took the region length to be $6'$ in our analysis of both the *Chandra* and *XMM-Newton* data (see Fig. 1) so that we could compare the fluxes using the exact same region. For consistency, we always use the same source and background regions in our analysis of both data sets. All errors on fluxes reported in this work are 95% confidence errors, errors on counts are at 1σ , and all other errors are at 90% confidence unless otherwise noted.

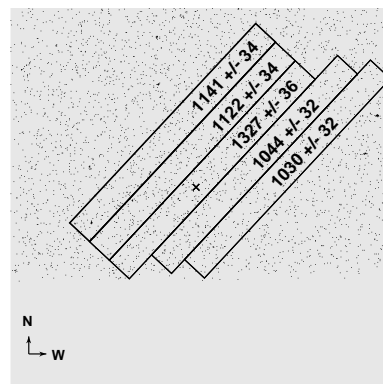
3. RESULTS

In its quiescent state, 4U 1755–33 remained undetected by *Chandra*. We obtain an upper limit for the flux of the LMXB by finding an average of 1.05 background counts in a $2''0$ radius circle, the size of the aperture that is expected to contain 90% of the flux for an on-axis ACIS point source at 1.49 keV. A source with less than five counts has a 3σ probability of being detected according to Poisson statistics; using a power-law model (with parameters equal to those we used to analyze the jetlike emission, described in detail below) with WebPIMMS³, this corresponds to a flux upper limit of 2.98×10^{-15} ergs $\text{cm}^{-2} \text{s}^{-1}$.

3.1. Emission from the Jetlike Region

In 2003, Angelini and White reported the detection of a $7'$ jetlike feature of extended emission, centered on the position of 4U 1755–33 and at a position angle of $\sim 137^\circ$. 4U 1755–33 is located off the galactic plane at RA $17^{\text{h}}58^{\text{m}}40^{\text{s}}0$ and DEC $-33^\circ48'27''.0$ ($l = 357^\circ21$, $b = -4^\circ87$), so the emission is not likely to be due to a feature in the plane. The emission is also found to be symmetric, as expected from a binary source observed at high inclination.

The jetlike feature is very prominent in the *XMM-Newton* images of Angelini and White (see Fig. 1 and Fig. 2 of their paper). In the high-resolution *Chandra* image, however, the jet is not visually apparent. The *Chandra* image provides evidence that the emission may be diffuse: a rectangular area of $0.6 \times 6'$ enclosing the expected jetlike feature contains many more counts than regions of identical area next to the jet region, as shown in Figure 2. The central region was found to have 1327 ± 36 counts, which is 4.1 sigma above the region directly to the northeast (with 1122 ± 34 counts) and 5.8 sigma above the region directly to the southwest (with 1044 ± 32 counts).



³ <http://heasarc.gsfc.nasa.gov/Tools/w3pimms.html>

FIG. 2.— *Chandra* region counts. The central rectangle, which is identical to the solid-line rectangle shown in Figure 1, encloses most of the jetlike feature observed with *XMM-Newton*. The four flanking rectangles enclose background comparison regions. The total number of counts detected after point source subtraction in each of the $0.6 \times 6'$ regions is indicated. As before, the “x” in the central rectangle marks the location of 4U 1755–33. The same rectangular regions were used in analyzing the *XMM-Newton* data.

The jet region has 244.4 ± 43.6 net counts using the two outer rectangles as the background region. (The lower 0.6 of the leftmost rectangle was excluded due to contamination by point source D – see Fig. 1). This background region is used for all analysis in this paper. (See Table 1 for a description of the counts recorded in various regions.) The local background appears to be relatively independent of location in the *XMM-Newton* data, whereas there is a significant variation in the *Chandra* background on the two sides of the central rectangle that contains the source. Spatial variations of this magnitude are frequently observed in ACIS images⁴. The standard ACIS-S3 background dataset from the calibration database (CALDB) showed the same ratio of variation between the sum of the two leftmost rectangles and the sum of the two rightmost rectangles, suggesting that the variation we see is not specific to our image.

We adopted the simple power-law and thermal bremsstrahlung models used by Angelini and White. For both models, we froze the hydrogen column density at $N_{\text{H}} = 3 \times 10^{21} \text{ cm}^{-2}$, which is the value predicted from H I maps in the direction and at the distance of 4U 1755–33 (Dickey & Lockman 1990; Fruscione et al. 1994), and is similar to the N_{H} values adopted by others (e.g. Seon et al. 1995). From our best fit power-law model, we obtained photon indices of 1.2 ± 0.4 for the *Chandra* data, and 1.6 ± 0.2 for the *XMM-Newton* data. These are also consistent with the photon index of 1.8 ± 0.3 found by Angelini & White (2003) using the same value of N_{H} . In the various models they adopt, Angelini and White find photon indices ranging from 1.5 to 1.9 for their jet region, which they note are similar to values observed from other galactic and extragalactic jets associated with black holes. In order to better constrain our model, we chose to freeze the power-law photon index at 1.5 in our determination of the flux. The temperature was also very poorly constrained in the bremsstrahlung model. Because we could not get a precise value for this parameter, and because Angelini and White report a lower limit of 4 keV in their analysis, we chose to constrain our model by freezing the temperature at 4 keV. Fixing the temperature at 4 keV or at 10 keV returned minimal differences in the fluxes found.

Our fits for the normalization parameter generated a reduced χ^2 of 1.03 and 0.30 for both models in *Chandra* and *XMM-Newton*, respectively. The $0.6 \times 6'$ jet region in the *XMM-Newton* image yielded an average unabsorbed flux of $0.96 \pm 0.34 \times 10^{-13} \text{ ergs cm}^{-2} \text{ s}^{-1}$ for the MOS-1 and MOS-2 cameras and $1.32 \pm 0.45 \times 10^{-13} \text{ ergs cm}^{-2} \text{ s}^{-1}$ in *Chandra* in the 0.3–7.0 keV band with the power-law model. (See Table 2 for a summary of these results and the results from the bremsstrahlung model.) These fluxes correspond to a luminosity of $1.83 \pm 0.65 \times 10^{32} d_{4\text{kpc}}^2 \text{ ergs s}^{-1}$ from the *XMM-Newton* data

and $2.51 \pm 0.86 \times 10^{32} d_{4\text{kpc}}^2 \text{ ergs s}^{-1}$ from the *Chandra* data.

3.2. Emission in the Knot Region

Two bright knotlike regions were found in the *XMM-Newton* image in the southeastern end of the emission area. They appear to be broader than the point-spread function (PSF) of *XMM-Newton* of $9''$ in radius at 1.5 keV for a region encircling half of the total energy. One of these regions was also imaged by *Chandra* (see Fig. 1). We analyzed this knot, at RA $17^{\text{h}}58^{\text{m}}46^{\text{s}}.64$ and DEC $-33^{\circ}49'49''.48$, using the same models described above. We selected a $24''$ diameter extraction aperture by comparing the net counts for a series of aperture sizes and noting where the flux fell off most significantly. The background region used was identical to the one described in our jet analysis.

The knot region had a greater concentration of net counts compared to the net counts in the region of jetlike emission in the *XMM-Newton* data, but the knot emission was not detected at a significant level in the *Chandra* data. *XMM-Newton* recorded 34.4 ± 7.2 net counts in the knot, which, when scaled for area, is greater than the average net counts in the jet region significant to 3.5σ . *Chandra* recorded 12.2 ± 7.1 net counts, which is not statistically different than the net counts recorded in the jet region. The unabsorbed 0.3–7.0 keV flux with the power-law model yielded an upper limit of $4.63 \times 10^{-14} \text{ ergs cm}^{-2} \text{ s}^{-1}$ from the averaged MOS cameras and $1.32 \times 10^{-14} \text{ ergs cm}^{-2} \text{ s}^{-1}$ from the *Chandra* data. See Table 1 for a description of the counts obtained in the knot region, and Table 2 for a summary of the fluxes found obtained from both the power-law and the bremsstrahlung models for the knot region.

4. DISCUSSION

The lack of visibility of the knot in *Chandra* suggests that the object may be diffuse. We verified this hypothesis by comparing the ratio of the fluxes between the knot and the jet in *XMM-Newton* and *Chandra*. Assuming that N_{H} and Γ are the same for both the knot and the jet, and that the flux of the knot has not changed significantly in the 2.5 years between the *XMM-Newton* and *Chandra* observations, the ratio between the net knot and jet flux in *XMM-Newton* gives a predicted 30.3 ± 9.0 net counts for the knot in *Chandra* for the 0.3–7.0 keV band. This method of scaling gives a count value for the knot that is different from the actual 12 ± 7.1 net counts of observed in the *Chandra* image by 1.58σ . Choosing harder energy bands makes the knot more significant: in the 4.0–7.0 keV band, the knot net counts is higher than the jet net counts by 3.0 ± 0.5 ; for the 0.3–7.0 keV band, the knot is only 1.4 ± 0.4 times higher. The surface brightness sensitivity of *Chandra* may be too low to statistically detect the a diffuse knot in the 0.3–7.0 keV band. If all of the counts in the knot had been concentrated at a point source, the knot would be significant and immediately apparent in the *Chandra* image, since the background in a typical $2''$ radius extraction aperture is only 1.05 counts in the 0.3–7.0 keV band (see Table 1). Thus, we suggest that the observed knot is most likely a real, but diffuse, feature.

Likewise, the jetlike emission is also likely a real feature. The agreement between the *Chandra* and *XMM-*

⁴ <http://cxc.harvard.edu/contrib/maxim/bg/index.html>

Table 1: **Region Counts**

	JET		KNOT		BACKGROUND
	Total Counts	Net Counts	Total Counts	Net Counts	Total Counts
<i>XMM-Newton</i>	782.0±28.0	277.8±32.4	52.0±7.2	34.4±7.2	958.0±31.0
<i>Chandra</i>	1327.0±36.4	244.4±43.6	50.0±7.1	12.2±7.1	2057.0±45.4
Region Size	0'6 × 6'		$\pi \times 0'.2^2$		(0'6 × 6') + (0'6 × 5.4')

Newton fluxes for the jet region suggest that the emission visibly seen in the *XMM-Newton* data must still be present in the *Chandra* data. Though the *Chandra* data had slightly longer good time exposure (~ 22000 s, compared to ~ 18100 s for the MOS cameras aboard *XMM-Newton*), there are other factors that have contributed to the lack of visibility of the jet in *Chandra*, including *XMM-Newton's* greater effective area: at 1.5 keV, the effective area of the MOS cameras aboard *XMM-Newton* is 1400 cm^2 compared to *Chandra's* 700 cm^2 . The background rates are also twice as high with *Chandra*, making significant detections of diffuse emission more difficult. Thus, if the emission were truly diffuse, it would have been more easily detected with the capabilities of the *XMM-Newton* instruments.

The emission is not likely to be due to an alignment of point sources, as multiple point sources were not found in the emission region by either *Chandra* or *XMM-Newton*. Six point sources located outside the jet region, which were detected by both *Chandra* and *XMM-Newton*, are shown in Figure 1 with their positions and net counts listed in Table 3. Of course, a large enough assemblage of very faint point sources would have escaped detection as individual sources (e.g., 100 or more source with fluxes of $\sim 10^{-15} \text{ ergs cm}^{-2} \text{ s}^{-1}$ or less), although this scenario is an unlikely one.

It is important to note that since one of the bright knotlike regions that was detected by *XMM-Newton* was off the S3 chip of *Chandra*, a simple scaling of the fluxes found in our analysis of the $0'.6 \times 6'$ region to the estimated true size of the jet of $7'$ may yield a slight underestimate of the actual flux in the region. However, since we cannot analyze the *Chandra* image with a $7'$ jet, we limited our *XMM-Newton* analysis to $6'$ regions for more accurate and consistent comparisons between the two telescopes.

5. CONCLUSIONS

While the *Chandra* image showed many point sources, emission from LMXB 4U 1755–33 in quiescence was not detected. We present the results of a comparative study using *Chandra* and *XMM-Newton* imaging data of a jet-like emission feature that is apparently emanating from 4U 1755–33. Although the jetlike feature is not directly visible in the *Chandra* image, though highly visible in the *XMM-Newton* images, *Chandra* does detect significant emission ($4\text{--}6\sigma$) from the jet region. Furthermore, we find that the fluxes from the same $0'.6 \times 6'$ jet region as observed by *Chandra* and *XMM-Newton* agree within errors. The flux of a knotlike region embedded in the jet was detected by *XMM-Newton*, but not by *Chandra* because of *Chandra's* smaller area and higher background. We show that if this emission were due to a point source, then it would have been easily detected by *Chandra*. We therefore conclude that the emission from the knot is diffuse. Our analysis shows that the jetlike emission surrounding 4U 1755–33 is likely a true and diffuse jet, which appears to be devoid of point-like regions of emission associated with internal shocks. Because jets evolve very rapidly in our galaxy, compared with the slowly evolving larger scale jets of quasars and AGN, studying the jets from 4U 1755–33 and other galactic sources may provide key information in understanding jet formation and propagation.

We thank W. Forman and M. Markevitch for discussions on the spatial structure of the ACIS background. J. M. M. acknowledges support from the NSF through its Astronomy and Astrophysics Postdoctoral Fellowship program. This work has made use of the information and tools available at the HEASARC Web site, operated by GSFC for NASA.

REFERENCES

- Angelini, L., & White, N. E. 2003, *ApJ*, 586, L71
 Arnaud, K. A., & Dorman, B. 2000, XSPEC is available via the HEASARC on-line service, provided by NASA/GSFC
 Dickey, J. M. & Lockman, F. J. 1990, *ARA&A*, 28, 215
 Frank, J., King, A., & Raine, D. J. 2002, *Accretion Power in Astrophysics* (3d ed.; Cambridge: Cambridge University Press), 398
 Fruscione, A., Hawkins, I., Jelinsky, P., & Wiercigroch, A. 1994 *ApJS*, 94, 127
 Giacconi, R., Murray, S., Gursky, H., Kellogg, E., Schreier, E., Matilsky, T., Koch, D., & Tananbaum, H. 1974, *ApJS*, 27, 37
 Jones, C. 1977, *ApJ*, 214, 856
 Mason, K. O., Parmar, A. N., & White, N. E. 1985, *MNRAS*, 216, 1033
 McClintock, J., Canizares, C., Hiltner, W. A., Petro, L., & Griffiths, R. 1978, *IAU Circ.*, 3251, 1
 Miller, J. M., et al. 2002a, *ApJ*, 570, L69
 Miller, J. M., et al. 2002b, *ApJ*, 578, 348
 Mirabel, I. F. 2003, *New Astronomy Review*, 47, 471
 Pan, H. C., Skinner, G. K., Sunyaev, R. A., & Borozdin, K. N. 1995, *MNRAS*, 274, L15
 Park, S. Q., et al. 2004, *ApJ*, 610, 378
 Roberts, M. S. E., Michelson, P. F., Cominsky, L. R., Marshall, F. E., Corbet, R. H. D., & Smith, E. A. 1996, *IAU Circ.*, 6302, 2
 Seon, K., Min, K., Yoshida, K., Makino, F., van der Klis, M., van Paradijs, J., Lewin, W. H. G. 1995, *ApJ*, 454, 463
 Tanaka, Y., & Lewin, W. H. G. 1995, *X-Ray Binaries*, ed. W. H. G. Lewin, J. van Paradijs, & E. P. J. van den Heuvel (Cambridge: Cambridge Univ. Press), 126
 Wachter, S., & Smale, A. P. 1998, *ApJ*, 496, L21
 White, N. E., & Marshall, F. E. 1984a, *ApJ*, 281, 354
 White, N. E., Parmar, A. N., Sztajno, M., Zimmermann, H. U., Mason, K. O., & Kahn, S. M. 1984b, *ApJ*, 283, L9
 Wise, M. W., Davis, J. E., Huenemoerder, D. P., Houck, J. C., & Dewey, D. 2003, *MARX 4.0 Technical Manual*

Table 2: Flux Limits For The Jet And Knot Regions

	JET REGION	KNOT REGION
Power-law Model		
<i>Chandra</i>	$1.32 \pm 0.45 \times 10^{-13}$	1.32×10^{-14}
<i>XMM-Newton</i>	$0.96 \pm 0.34 \times 10^{-13}$	4.63×10^{-14}
Bremsstrahlung Model		
<i>Chandra</i>	$1.07 \pm 0.37 \times 10^{-13}$	1.07×10^{-14}
<i>XMM-Newton</i>	$0.86 \pm 0.31 \times 10^{-13}$	4.01×10^{-14}

Table 3: Point Source Positions

ID	RA	DEC	Net Counts
A	17 58 44.24	-33 45 09.52	77
B	17 58 44.06	-33 46 11.83	54
C	17 58 46.81	-33 48 44.74	43
D	17 58 51.17	-33 49 13.58	89
E	17 58 20.99	-33 46 53.50	97
F	17 58 20.15	-33 49 04.03	15